

# Dissipative hydrodynamic interactions via lattice-gas cellular automata

Anthony J. C. Ladd

Lawrence Livermore National Laboratory, Livermore, California 94550

Daan Frenkel

FOM-Institute for Atomic and Molecular Physics, 1009 DB Amsterdam, The Netherlands

(Received 4 June 1990; accepted 31 July 1990)

A three-dimensional lattice-gas model has been used to determine the dissipative hydrodynamic interactions between spherical particles. When the particles are close together the accuracy of the lattice-gas simulations is superior to typical integral-equation solutions of the creeping-flow equations. Moreover, the computational requirements scale linearly with system size, instead of quadratically or cubically. A new set of microrules have been implemented, which simulate a constant-velocity, no-slip boundary condition at the solid-fluid surfaces. Numerical results for various drag coefficients are reported.

The interaction of slowly moving solid particles with an incompressible fluid is a complex problem, with applications in many areas of chemistry and physics.<sup>1</sup> Analytic calculation of these hydrodynamic interactions is only possible in asymptotic regions; when the particles are nearly touching (lubrication) and when they are widely separated. Consequently, numerical calculations of hydrodynamic interactions, usually based on discretized solutions of the Oseen equation, are becoming more common.<sup>2</sup> However, accurate calculations of the hydrodynamic transport coefficients necessitate solving large, dense sets of simultaneous equations, of the order of 100–200 equations per particle at high density;<sup>3</sup> this severely limits the system sizes that can be studied. Recently we suggested that a lattice-gas cellular automata could be a computationally attractive method of simulating the hydrodynamic interactions between suspended solid particles.<sup>4</sup> In cases where Brownian motion is important, lattice-gas models possess the fundamental advantage that thermal fluctuations are implicitly included; whereas in conventional Navier–Stokes methods they must be added on after the dissipative interactions have been calculated. The addition of Gaussian random noise to a purely dissipative Navier–Stokes calculation has two disadvantages. First, it is very expensive; the computational effort to compute the covariance matrix, from which the random velocities or displacements are sampled, grows as the cube of the system size, if hydrodynamic interactions are to be included. Second, non-Gaussian effects, which give rise to experimentally interesting phenomena at short times,<sup>5</sup> are omitted. By contrast, recent simulations of the diffusion of a solid particle, suspended in a lattice gas,<sup>6</sup> confirm that lattice-gas models reproduce the algebraic decay of the velocity correlation function observed in Ref. 5.

Our simulations were run in three dimensions, projecting the four-dimensional face-centered-hypercubic (FCHC) lattice gas<sup>7</sup> onto a three-dimensional subspace to ensure isotropy. All the simulations were run at one-half the maximum density of the lattice gas (12 lattice-gas particles per node on average), so that its macroscopic behavior is described by the linearized Navier–Stokes (creeping-flow) equations.<sup>7</sup> We used the collision rules described in

Ref. 8, which lead to an exactly isotropic viscosity  $\eta = 1.23(m/l \Delta t)$ , where  $m$  is the mass of the lattice-gas particles,  $l$  is the lattice spacing, and  $\Delta t$  is the time step. Boundary conditions in a lattice gas are implemented by microrules that are local to each node. For stationary objects we use the usual “bounce-back” rule for the hydrodynamic stick boundary condition; for moving objects we use a generalization of this rule, which allows some particles to leak through the boundary surface in the direction of the local motion.<sup>8</sup> The flux of particles through the surface is dependent only on the local velocity; but surprisingly, the hydrodynamic modes apparently persist right up to the boundary surface with no microscopic boundary layer.

The constant-velocity boundary condition is implemented as follows. First, the solid particle surface is mapped as closely as possible onto the lattice; but ensuring that there are no direct links connecting the interior and exterior volumes of the solid particle. The local velocity at each boundary node is then computed from the translational and rotational velocity of the solid particle. The microrules at the boundary nodes are comprised of independent rules for each pair of velocity directions,  $c_i$  and  $c_{-i} = -c_i$  with  $i$  ranging from 1 to  $b/2$ , where  $b$  is the total number of velocity directions. We arbitrarily choose the link direction  $i$  so that  $X_i = (\mathbf{u} \cdot \mathbf{c}_i)/c^2 > 0$ , where  $\mathbf{u}$  is the velocity of the node. For a stationary node, particles with velocity  $c_i$  are reflected into particles with velocity  $c_{-i}$  and vice versa. To implement a constant-velocity boundary condition, a small fraction  $p_i$  of the particles moving in the  $i$  direction are allowed to remain undisturbed, while the remainder of these particles and all those moving in the  $-i$  direction are reflected. The transmission probability  $p_i$  is chosen so that the velocity distribution at the node is characteristic of the local velocity of the solid particle surface  $\mathbf{u}$ . For the FCHC lattice gas at a density  $\rho = mb/2$ , the expression for  $p_i$  is<sup>8</sup>

$$p_i = 16X_i / (1 + 4X_i)^2. \quad (1)$$

It can be shown that to third order of smallness ( $\mathbf{u}\mathbf{u}\mathbf{u}$  and  $\nabla\mathbf{u}\mathbf{u}$ ) the transmission probability,  $p_i$  [Eq. (1)], is unaffected by velocity gradients; this implies that the hydrody-

TABLE I. Drag coefficients for periodic arrays of spheres; details of the simulations are given in the text. Results are characterized by the radius of the solid particles ( $a$ ) and the length of the one-particle unit cell ( $L$ ); the effective packing fraction ( $\phi$ ) is also shown. The coefficients  $\zeta$  measured in each simulation are normalized by the theoretical coefficients  $\zeta_{Th}$ , which are determined from precise numerical solutions of the creeping-flow equations. The drag coefficients relative to an isolated sphere vary widely as a function of packing fraction: for  $\zeta^D$  this ratio varies from 1 to about 40, for  $\zeta^H$  it varies from 1 to about 100, and for  $\zeta^L$  and  $\zeta^R$  it varies from 1 to about 4.

$a$	$L$	$\phi$	$\zeta_F^D/\zeta_{Th}^D$	$\zeta_M^D/\zeta_{Th}^D$	$\zeta^H/\zeta_{Th}^H$	$\zeta^L/\zeta_{Th}^L$	$\zeta^R/\zeta_{Th}^R$
4.57	16	0.098	0.99		0.99	1.00	0.99
	11	0.300	0.98				
8.65	30	0.100	1.00	0.99	0.99	1.00	1.01
	21	0.293	1.00	0.97	0.98	1.00	1.01
	18	0.465		0.96	0.95	1.03	1.05
16.66	57	0.105	1.01	0.99	1.00	0.98	0.99
	51	0.146			1.00	1.00	
	46	0.199			0.99	1.00	
	40	0.303	0.99	0.99	0.99	0.99	0.99
	36	0.415			0.98	0.98	
	35	0.452			0.98	1.00	
	34	0.493		0.98	0.88	0.98	1.00
32.66	78	0.308	1.00	1.00	1.00	0.98	
	67	0.485			0.96	1.01	
	66	0.508		1.00	0.84	1.00	1.02

dynamic modes persist right up to the solid boundary, without an intervening boundary layer. Solutions of the lattice Boltzmann equation for mixed slip-stick boundary conditions, using similar looking microrules, have also shown an absence of boundary layers.<sup>9</sup> As we shall see, the numerical results reported here also support the conclusion that there is no microscopic boundary layer; much larger solid particles would be required for quantitative results if boundary layers were present. These new microrules are a fundamental improvement over our previous implementation of a moving boundary condition,<sup>4</sup> which almost certainly set up boundary layers around the solid particles. Moreover, the new rules are much simpler to implement. The fluid fills the whole of the space, both inside and outside the solid particles, and it is therefore straightforward to move the center of mass of the solid particle from one node to another; only the map of the boundary nodes on the lattice needs to be changed. When a particle is moving, small amounts of fluid leak through the boundary surface in the direction of the solid particle motion. Theoretically, the velocity field inside the particle should be uniform and equal to the particle velocity; we have verified numerically that this is indeed so, on average.

An essential check of the applicability of lattice-gas models to problems involving solid-fluid interactions is that they should accurately and efficiently simulate the dissipative hydrodynamic interactions between suspended solid particles. The focus of this work has been a comparison of the dissipative hydrodynamic forces derived from lattice-gas simulations with precise numerical solutions of the creeping-flow fluid equations. Thus we have been able to quantitatively assess the accuracy of lattice-gas models, as a function of the solid particle size relative to the lattice spacing. The first two sets of experiments were aimed at calculating the drag force exerted by a fluid flowing over a stationary, simple-cubic lattice of spheres, and the drag force exerted by the same array of spheres moving through a stationary fluid. If the system is Galilean invariant mac-

roscopically, then these two drag coefficients,  $\zeta_F^D$  and  $\zeta_M^D$ , respectively, should be the same. Our simulations consisted of cubic unit cells containing a single sphere at the center. By varying the radius of the sphere we covered a range of packing fractions  $\phi$  from fairly dilute ( $\phi = 0.1$ ) to concentrated ( $\phi = 0.5$ ). The unit cells were periodic in two dimensions and several such cells, identical macroscopically, but with different microscopic states of the lattice gas, were chained together in the remaining, nonperiodic, direction. Boundary conditions were applied at the ends of the chain of cells: in the first set of experiments a density difference was used to drive the fluid over stationary spheres, in the second set of experiments the "bounce-back" rule was used to simulate a stationary wall. The flow velocity and drag force were measured only in the central cell; the remaining cells were used to ensure that the central cell had the periodic inflow and outflow boundary conditions. By increasing the number of cells in the chain, the effects on the central cell of the boundary conditions at the ends of the chain could be eliminated. The drag coefficients determined by this procedure converge rapidly to a limit characteristic of a simple-cubic lattice; typically we see no significant change in the drag coefficients for chains longer than five unit cells, although in some instances we have used chains of seven or nine unit cells. The density difference across the chain of cells was typically of the order of 1%–10% and was always sufficiently small for the linear response to be extracted. Similarly, in the case of the moving spheres, the sphere velocity was sufficiently small so that the response was again linear; a typical solid-particle velocity would be 1% of the lattice-gas particle speed. The particles do not actually move their center of mass in these simulations; the diffusion of colloidal particles is so slow that it does not, in general, couple with the relaxation of velocity. Results for these drag coefficients are compared in Table I with essentially exact solutions of the creeping-flow equations for the same macroscopic geometry (i.e., a simple-cubic lattice).<sup>10</sup> It can be seen that the agreement is

very good, within 1%–2% over the whole density range, even for spheres with a radius of a few lattice spacings. This is within the range of the statistical fluctuations, which after simulations of  $10^4$  to  $10^5$  time steps are of the order of 1%. It should be noted that it is not possible to assign the effective hydrodynamic radius of the solid particle *a priori*. We would expect the stick boundary condition to apply midway between the boundary nodes and the nearest fluid nodes, so that the hydrodynamic radius should be roughly the average radius of the boundary nodes plus half a lattice spacing. The measured hydrodynamic radius  $a$ , determined from the low-density drag coefficients, is slightly larger; by between 0.1 and 0.2 lattice spacings. All the simulations for a particular size sphere use the same value of the hydrodynamic radius, and the difference between the hydrodynamic and average radii varies little from one size sphere to another (Table I).

A more stringent test of the lattice-gas models occurs when there is relative motion between the solid particles. In such cases there are singular lubrication forces when the particles are close to touching; forces along the line of centers diverge as  $s^{-1}$  and forces perpendicular to the line of centers diverge as  $\ln s^{-1}$ , where  $s = (R_{12} - 2a)/a$  is the gap between the particles relative to the radius. The lattice-gas simulations comprised a chain of two cubic cells, similar to those described above. The particles in the cells moved with opposite velocities  $u$  and  $-u$ , and since there is no net momentum flux, the two ends of the chain were connected by periodic boundary conditions. For small enough velocities, the response (i.e., drag force versus velocity) was linear and superposable. These results are compared in Table I with integral-equation calculations, which include an explicit and exact calculation of the lubrication forces. Again the agreement is very good. For the logarithmically diverging force, perpendicular to the line of centers, we see no significant discrepancies (in  $\zeta^{\perp}$ ) down to a gap of  $0.02a$ . However, for the parallel force, diverging as  $s^{-1}$ , we obtain quantitative agreement (in  $\zeta^{\parallel}$ ) only for gaps greater than about one lattice spacing. Bulk properties of a suspension of such particles, which sample all distances, will be less sensitive to the short-range interactions than the single-configuration results reported here. Of course we could always include a separate calculation of the lubrication interactions, as was done for the integral-equation calculations, but this would complicate the calculation of the fluctuating forces. In any case it appears to be unnecessary, as can be seen from Fig. 1, where lattice-gas and integral-equation results for the parallel force are compared. On this scale the errors in the lattice-gas simulations are barely noticeable, since they correspond to very small shifts in the effective radius of the particle, of the order of 0.1 lattice spacings. These results suggest that a sphere radius of the order of ten lattice spacings should be large enough for most simulations of many-particle suspensions; simulations of several hundred such spheres are possible on modern supercomputers.

Finally, we have calculated the rotational drag coefficient ( $\zeta^R$ ) of a simple-cubic lattice of spheres, which also has a logarithmic singularity at high packing fractions. The

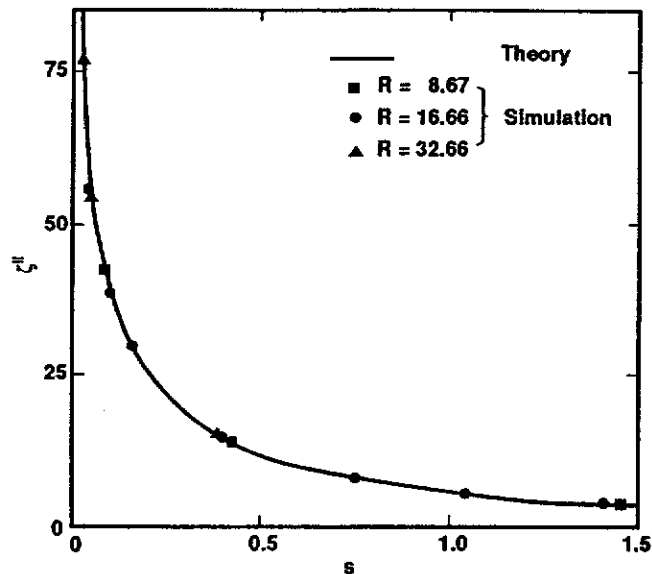


FIG. 1. Drag coefficient for spheres moving in opposite directions along their line of centers. The force on each sphere  $\pm F$  is normalized by the Stokes drag force so that  $\zeta^{\parallel} = F/(6\pi\eta aU)$ . The drag coefficients are plotted against the interparticle gap measured relative to the particle radius,  $s = (R_{12} - 2a)/a$ . The solid line is the theoretical result derived from an integral equation solution of the creeping-flow equations; the solid symbols are results from the lattice-gas simulations with spheres of various radii.

simulations used a single fully periodic unit cell, with a sphere rotating about a single axis. Again the agreement between lattice-gas and creeping-flow models is excellent over the whole density range.

At present we are testing the fluctuating forces induced by the lattice gas on a periodic array of spheres. The rates of translational and rotational diffusion of the spheres are consistent with the translational and rotational friction coefficients reported here. Thus it seems likely that lattice-gas cellular automata will become a useful and powerful tool for investigating two-phase solid–fluid flows, at least at low Reynolds number.

#### ACKNOWLEDGMENTS

We would like to acknowledge helpful discussions with Andy Masters (University of Manchester) and Rémi Cornubert (Ecole Normale Supérieure).

This work was supported by the U.S. Department of Energy and Lawrence Livermore National Laboratory under Contract No. W-7405-Eng-48. The work of the FOM Institute for Atomic and Molecular Physics is part of the research program of FOM and is supported by the "Nederlandse Organisatie voor Zuiver Wetenschappelijk Onderzoek."

<sup>1</sup>J. Happel and H. Brenner, *Low-Reynolds Number Hydrodynamics* (Nijhoff, Dordrecht, 1986).

<sup>2</sup>J. F. Brady and G. Bossis, *Annu. Rev. Fluid Mech.* **20**, 111 (1988).

<sup>3</sup>A. J. C. Ladd, *J. Chem. Phys.* **93**, 3484 (1990).

<sup>4</sup>A. J. C. Ladd, M. E. Colvin, and D. Frenkel, *Phys. Rev. Lett.* **60**, 975 (1988).

<sup>5</sup>D. A. Weitz, D. J. Pine, P. N. Pusey, and R. J. A. Tough, *Phys. Rev. Lett.* **63**, 1747 (1989).

<sup>6</sup>M. A. van der Hoef, D. Frenkel, and A. J. C. Ladd (unpublished, 1990).

<sup>7</sup>U. Frisch, D. d'Humières, B. Hasslacher, P. Lallemand, Y. Pomeau, and J-P. Rivet, *Complex Syst.* **1**, 649 (1987).

<sup>8</sup>A. J. C. Ladd and D. Frenkel, *Cellular Automata and Modeling of*

*Complex Physical Systems*, edited by P. Manneville, N. Boccara, G. Y. Vichniac, and R. Bidaux (Springer, Berlin, 1989).

<sup>9</sup>R. Cornubert, D. d'Humières, and C. D. Levermore, *Physica D* (in press).

<sup>10</sup>A. J. C. Ladd, *J. Chem. Phys.* **88**, 5051 (1988).